

VAPOR-LIQUID PHASE SEPARATION OF HE II

S. W. K. Yuan¹, A. R. Urbach², S. M. Volz², and J. H. Lee²

1 BEI Technologies, 13100 Telfair Avenue

Sylmar, CA 91342

Tel: (818) 364-7204, FAX: (818) 362-2487

2 Ball Aerospace & Technologies Corp.

Boulder, CO 80306

ABSTRACT:

A theory is proposed which uses both the permeability and bubble point diameter of the porous plug to characterize the full range operation of the Vapor Liquid Phase Separation (VLPS) of liquid helium. A computer model has been written based on the theory presented in this paper, which gives good correlation with VLPS data in the literature. The predicted performance of the SIRTf flight plug is also presented.

INTRODUCTION:

Vapor-Liquid phase separation (VLPS) using porous media was studied extensively during the late 70's and early 80's. After the Infrared Astronomical Satellite (IRAS) mission¹ there have been limited efforts in the research of the VLPS. The COBE mission² raised some uncertainty in the

operation of the phase separator as the temperature downstream of the porous plug was seen to fluctuate with time. The Superfluid Helium On-Orbit Transfer (SHOOT) experiment³ demonstrated the operation of a high vent rate VLPS system. Recently, the Jet Propulsion Lab conducted experiments⁴ on the phase separator to be used for the SIRTf mission. Despite these efforts, there is still quite a bit of discrepancy among various theories. Choked flow and hysteresis were not detected in a number of early studies of the VLPS. Whether these investigators overlooked the choked regime is not clear. Also, with the same permeability (which has been accepted as a more accurate parameter to characterize VLPS), some plugs tend to choke at higher flowrates than others. We hope that the theory presented in this paper will shed some light on the subject.

THEORY:

Generally speaking, the operating condition of the Vapor-Liquid Phase Separator can be divided into the Normal Operating Regime, the onset to Choked Flow, Fully Developed Turbulent Flow, and the Breakthrough Regimes.

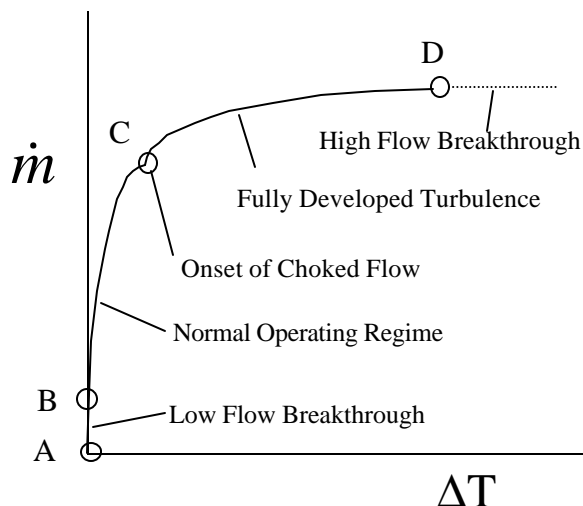


Figure 1. Transport regimes in a vapor-liquid phase separator, mass flow versus temperature difference across porous plug.

Normal Phase Separation Regime

In this regime (B-C in Figure 1), the vapor-liquid interface does not recede into the porous plug. It was mentioned in an earlier paper⁵ that the transport in this regime is not always linear. In the linear portion, the mass flow is linearly proportional to the temperature gradient across the porous plug⁶ and can be expressed as

$$\dot{m} = \frac{\rho^2 S^2 T K_p A \nabla T}{(1 + ST)\eta_n} \quad (1)$$

where ρ is the density, S is the entropy, λ is the latent heat of vaporization, T is the temperature, and η_n is the viscosity of the normal fluid. K_p is the permeability and A is the area of the plug. NASA Goddard⁷ reported good correlation between the linear data of COBE and Equation 1 at small flow rates. Equation 1 is also known as the Hagen-Poiseuille Equation (for pipe flow, $K_p=D^2/32$) or the Darcy Law (for porous media).

As the mass flow increases the transport turns into the transition regime, where the mass flow is no longer linearly proportional to the temperature gradient. This is supported by the data from Reference 4 and 8. If the porous plug chokes (see next section) before the formation of vortices, then the transition regime might not be observed.

The Normal Phase Separation regime is the desired operating regime of a VLPS, because of its predictability, with neither liquid breakthrough nor hysteresis due to choked flow.

The Choked Flow Limit

Choked flow in He II (C in Figure 1) was first explored experimentally by Murakami et al.⁸. DiPirro⁹ offered a simplified model for choked flow, hypothesizing that the vapor-liquid interface recedes into the porous plug, resulting in excessive temperature drop. Lages¹⁰ postulated a more complete theory for choked flow based on the Gibbs free energy analysis, which boils down to DiPirro's equation⁹, for pore sizes on the order seen in VLPS. In DiPirro's model, the temperature difference is given by

$$\Delta T = \frac{\frac{4\sigma}{D_c} + rgh}{rS - \left. \frac{dP}{dT} \right|_{svp}} \quad (2)$$

where σ is the surface tension, h is the height of the liquid and D_c is the equivalent capillary diameter. In combining Equation 1 and 2, one can predict the onset of the choked flow. Since choked flow begins at the largest pores and the bubble-point-pressure-test measures the diameter of the largest pores near the surface of the plug, we propose to substitute the equivalent capillary diameter in Equation 2 with the bubble point,

$$D_c = 4\sigma / \Delta P \quad (3)$$

where ΔP is the bubble point pressure.

The Fully Developed Turbulent Regime

The onset of choked flow as described above is referred to by many as the ‘knee’ (C in Figure 1). Beyond the knee, the transport is observed to be nonlinear. The choked flow equation predicts a flat profile of mass flow versus ΔT , which tends to under-predict the mass flow rate. Yuan⁶ on the other hand had great success in correlating literature data in this regime with the Gorter-Mellink Equation. He found that the mass flow is a strong function of the permeability or the pore size of the plug.

The onset of choked flow is likely to trigger the fully developed turbulent transport in the plug (C-D in Figure 1). The size dependence of the mass flow in this regime is attributed to the different onset points of the choked flow due to the pore size difference in Equation 2.

For fully developed Gorter-Mellink transport, the mass flow is proportional to the cube root of the temperature gradient

$$\dot{m} = \frac{AK_{GM}h_n r_s T}{l} \left(\frac{r^2 r_s S \nabla T}{r_n h_n^2} \right)^{1/3} \quad (4)$$

where the subscript s and n stand for the superfluid and normal fluid components, A is the area of the porous plug. K_{GM} is the Gorter-Mellink constant; a value of 0.014 was used in all calculations (i.e., with the present theory, the turbulent transport of He II in a porous plug is no longer size dependent as Yuan had found⁶). The Gorter-Mellink constant K_{GM} , is related to the more familiar Gorter-Mellink coefficient A_{GM} , by the following equation¹¹

$$K_{GM} = (\rho/\rho_s A_{GM} \eta_n)^{1/3} \quad (5)$$

Due to the tendency of the vapor-liquid interface to recede into the porous plug, hysteresis is sometimes observed in this regime. If the vapor-liquid interface recedes into the plug, Equation 4 is no longer valid and the temperature drop across the plug increases tremendously due to the presence of a vapor layer. In other words, Equation 4 is the upper limit of the hysteresis curve.

Liquid Breakthrough Regimes

Liquid breakthrough can occur at any time if the hydrostatic pressure plus the surface tension is larger than the fountain pressure ($\rho S \Delta T$). Breakthroughs are of particular concern at low and high flow rates.

Low flow breakthrough

In this regime (A-B in Figure 1), due to the small temperature difference across the plug, the phase separator is susceptible to liquid breakthrough, especially with the presence of a parasitic heat load at the downstream of the plug. The amount of flow can be calculated as follow

$$\dot{m}_b = Q / (I + ST) \quad (6)$$

where Q is the downstream parasitic heat. Since the downstream of the plug is cooled by the vaporization of liquid helium, the parasitic heat load is intercepted. This prevents further liquid breakthrough as the transport enters the Normal Operation Regime (B-C in Figure 1). Breakthrough is generally not a concern in this regime, unless the parasitic heat leak down the vent line is big.

High flow breakthrough

Due to the high flow rates, breakthrough in this regime (beyond D in Figure 1) can be catastrophic. However, this regime is seldom encountered in space because of the small hydrostatic head (liquid breakthrough occurs if the hydrostatic pressure plus the surface tension is larger than the fountain pressure, $\rho S \Delta T$, see Equation 2).

THE COMPUTER MODEL

Due to the highly non-linear nature of the equations and the sensitive temperature dependency of the properties, a computer model is developed to solve the equations. The Continuous System Simulation Language (CSSL)¹² has been used because it lends itself to solving large numbers of highly non-linear equations simultaneously.

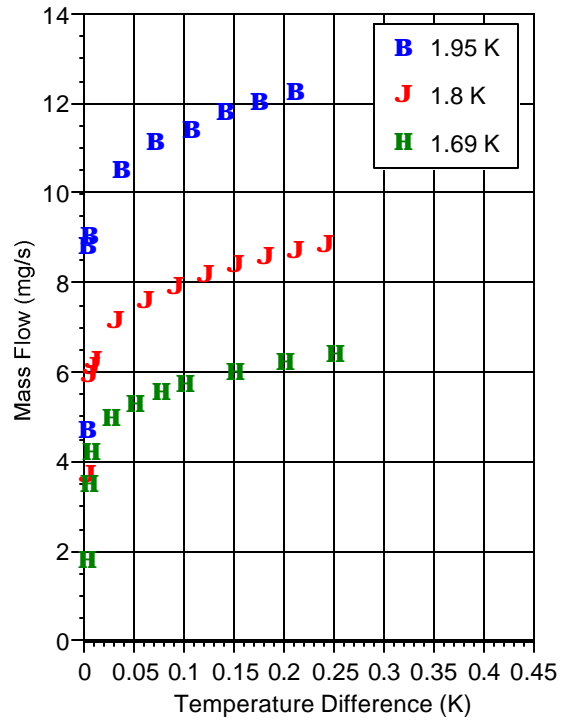
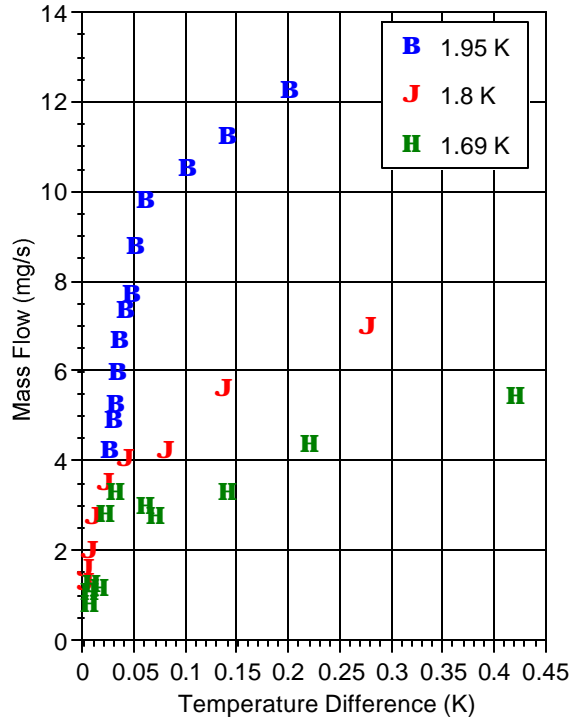
RESULTS AND DISCUSSIONS:

The model is compared to various VLPS data in the literature, including the IRAS plug, the COBE plug, and the data collected by JPL on the SIRTf plug. Table 1 summarizes the important parameters used in the computer model.

The experimental and predicted performance of the IRAS plug, the COBE plug and the JPL SIRTf plug are plotted in Figures 2 to 4 respectively. Within data scatter, the model gives good correlation to the experimental data.

Table 1. Important VLPS parameters used in the study.

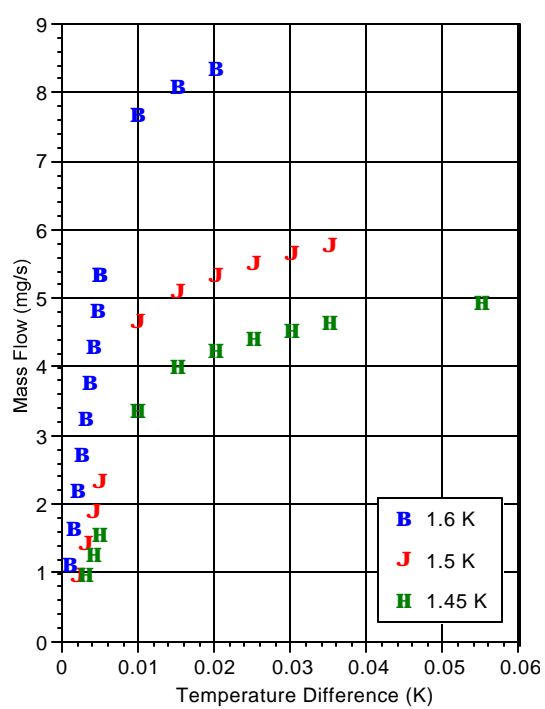
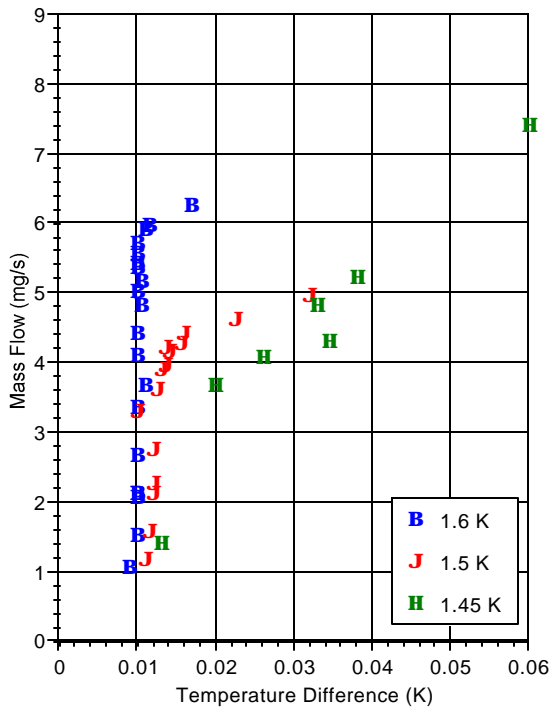
	Diameter (cm)	Thickness (cm)	Permeability (cm ²)	Porosity	Bubble Pt. Pore Size (μm)
IRAS	1.95	0.635	1E-9	0.380	3.9
COBE	3.30	0.635	1E-9	0.380	3.9
SIRTf (JPL)	7.74	0.635	5.4E-10	0.380	4.7
SIRTf (Ball)	3.81	0.635	1.4 E-9	0.249	2.8



(a)

(b)

Figure 2. (a) Experimental and (b) predicted performance of the IRAS plug.



(a)

(b)

Figure 3. (a) Experimental and (b) predicted performance of the COBE plug.

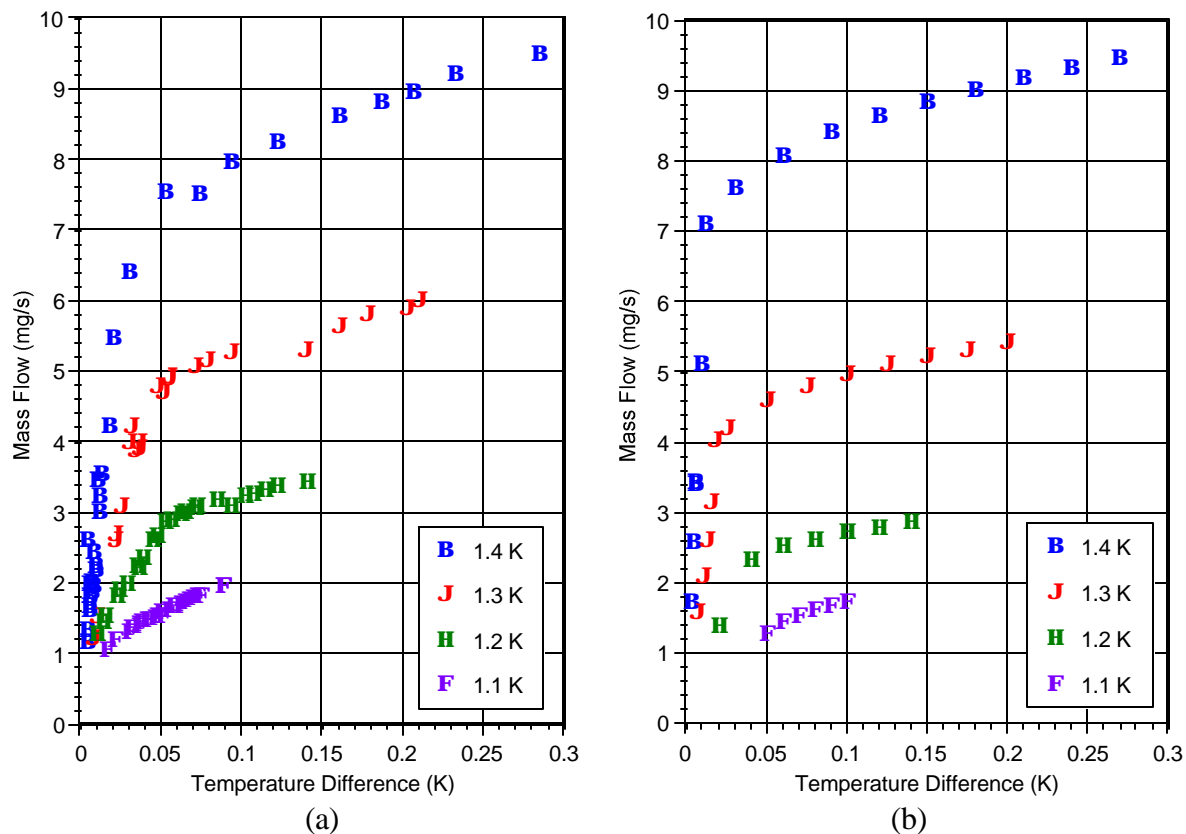


Figure 4. (a) Experimental and (b) predicted performance of the JPL SIRTf Plug. The predicted onset of the choked flow regime (or the knee) is listed in Table 2 together with the experimental result of the COBE plug. Excellent agreement is found between the two.

Table 2. Critical mass flow of the COBE plug.

Temperature (K)	Experimental Mc (mg/s)	Predicted Mc (mg/s)
1.45	3.2	3.2
1.50	4.1	4.0
1.60	6.0	6.4

Predicted Performance of the SIRTf Plug

With this computer model, one can then proceed to predict the performance of the SIRTf flight plug. Important parameters of this plug can be found in the last row of Table 1. The bubble point diameter of the Ball SIRTf plug was calculated to be 12.3 microns using Equation 3, and 2.8 microns based on an equation supplied by the plug manufacturer. The analysis in this paper was performed assuming the former bubble point diameter (worst case). Figure 5 shows the full operating range of the SIRTf plug for various bath temperatures. The SIRTf plug appears to be well designed as both the high flow (beginning of the mission) and low flow (normal operating condition) fall within the Normal Operating Regime, as shown in Figure 6. Due to the high permeability and large surface area of the plug, the predicted temperature difference across the plug (in Figures 5 and 6) is extremely small. To avoid this, it is recommended to reduce the diameter of the plug to a smaller size. The maximum throughput of this plug is plotted in Figure 7, assuming 1 torr and 3 torr pressure drop in the vent line.

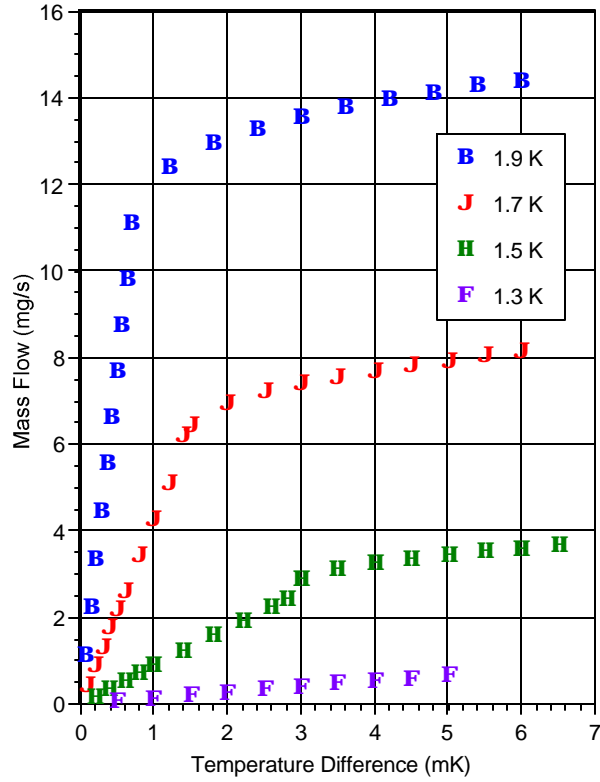


Figure 5. Full operating range of the SIRTf flight plug.

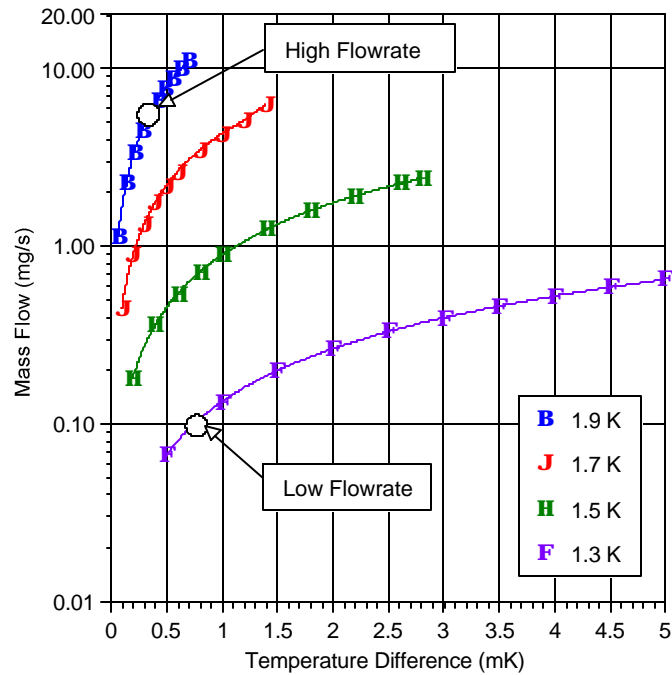


Figure 6. Normal operating range of the SIRTf flight plug.

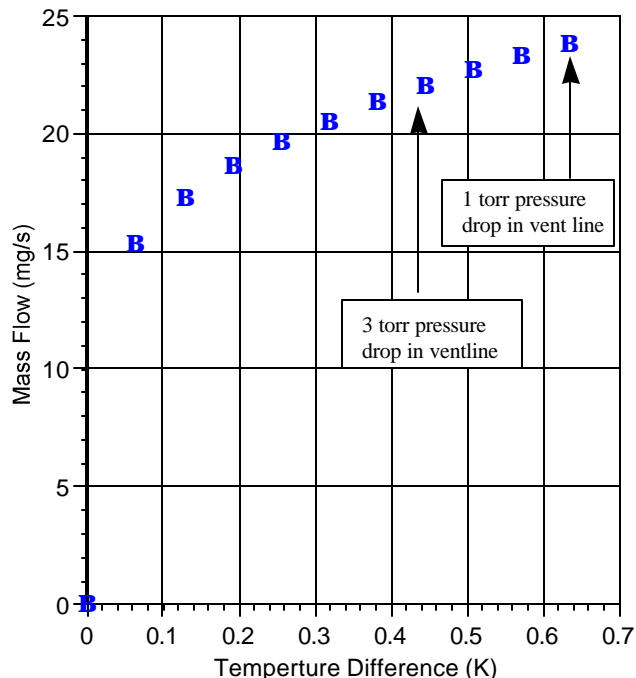


Figure 7. Maximum throughput of the SIRFT flight plug.

CONCLUSIONS:

The theory behind the full operating range of a vapor-liquid phase separator is presented in this paper. Based on the theory, a computer model has been constructed which gives good correlation (within uncertainty of the bubble point diameter measurement, permeability measurement, and distribution of pore size) to the VLPS data in the literature for a wide range of plug geometry, permeability, and bath temperature. This supports the proposed theory that the upper branch of the hysteresis loop is governed by the fully developed turbulent flow of the Gorter-Mellink Equation, which is triggered by the onset of choked flow. The bubble point diameter (in Equation 3) was found to be a critical parameter that should be used in place of the capillary diameter in Equation 2 to predict the onset of the choked flow.

REFERENCES:

- 1) D. Petrac and P.V. Mason, *Adv. Cryo. Eng.*, 29:661 (1983).
- 2) S.M. Volz, M.J. DiPirro, S.H. Castles, M.G. Ryschkewitsch, and R. Hopkins, *Adv. Cryo. Eng.*, 37b:1183 (1992).
- 3) J.G. Tuttle, M.J. DiPirro and P.J. Shirron, *Adv. Cryo. Eng.*, 39:121 (1994).
- 4) D. Elliott, JPL report, JPL D-11412 (1994).
- 5) S.W.K. et. al., *Adv. Cryogenic Engineering*, 41:1189 (1996).
- 6) S.W.K. Yuan, Ph.D. Thesis, University of California, in Los Angeles (1985)
- 7) M.J. DiPirro, private communication.
- 8) M. Murakami et al., The (Japanese) Institute of Space and Astronautical Science Report No. 612 (1984)
- 9) M.J. DiPirro and J. Zahniser, *Adv. Cryo. Eng.*, 35:173 (1990).
- 10) C.R. Lages, R.H. Torii, and D.B. Debra, *Cryogenics* 35:33 (1995).
- 11) S.C. Soloski, Ph.D. Dissertation in Engineering, University of California, Los Angeles, (1977).
- 12) Continuous System Simulation Language (CSSL), Simulation Services, a division of Nilsen Associates, Chatsworth, CA 91311.